

Optimal control of quasi-1D Bose gases in optical box potentials

A. Deutschmann-Olek* K. Schrom* N. Würkner*
J. Schmiedmayer** S. Erne** A. Kugi*,***

* *Complex Dynamical Systems Group, Automation and Control
Institute, TU Wien, Vienna, Austria*

** *Vienna Center for Quantum Science and Technology, Atominstytut,
TU Wien, Vienna, Austria*

*** *Center for Vision, Automation & Control, Austrian Institute of
Technology, Vienna, Austria*

Abstract: In this paper, we investigate the manipulation of quasi-1D Bose gases that are trapped in a highly elongated potential by optimal control methods. The effective mean-field dynamics of the gas can be described by a one-dimensional non-polynomial Schrödinger equation. We extend the indirect optimal control method for the Gross-Pitaevskii equation by Winckel and Borzi (2008) to obtain necessary optimality conditions for state and energy cost functionals. This approach is then applied to optimally compress a quasi-1D Bose gas in an (optical) box potential, i.e., to find a so-called short-cut to adiabaticity, by solving the optimality conditions numerically. The behavior of the proposed method is finally analyzed and compared to simple direct optimization strategies using reduced basis functions. Simulations results demonstrate the feasibility of the proposed approach.

Keywords: Optimal control, partial differential equations, non-polynomial Schrödinger equation, Bose gases, ultra cold atoms

1. INTRODUCTION AND MOTIVATION

Recent progress in quantum experiments vastly improved the capabilities of controlling and manipulating individual quantum systems and laid the foundation for future technologies that try to harness genuine quantum effects to fulfill desired tasks with superior performance. Observing and exploiting quantum effects experimentally is a notoriously hard problem due to the fragility of quantum states in their natural surrounding. Suppressing disturbances and other detrimental effects on the system behavior is a classical task in control engineering. As a consequence, methods from automatic control and control engineering have proven highly valuable to achieve such goals, see, e.g., Grond et al. (2009); Dotsenko et al. (2009); Omran et al. (2019); Magrini et al. (2021), and are expected to become vital building blocks for quantum technologies.

A particularly versatile model platform to explore and utilize quantum many-body systems are trapped clouds of ultra-cold atoms that form Bose gases. The reliable manipulation of atomic clouds on Atom chips suggested the use of optimal control methods to optimize the handling of trapped Bose-Einstein condensate in one and three dimensions, see Grond et al. (2009); Mennemann et al. (2015). Recent interest in quantum-thermodynamic questions and the lack of suitable experimental platforms stimulated the investigation of thermal machines operating on quantum fields. Thereby, an ultra-cold atomic cloud in a highly elongated trap is used as a working fluid. This quasi-1D Bose gas is then manipulated in longitudinal direction, i.e., the weakly confined direction, to implement desired

thermal operations. Since such operations introduce unwanted heat to the gas in general, it seems natural to use optimal control methods to mitigate such heating effects. The finite temperature case of the quantum many-body system would require a description of the quantum field's stochastic fluctuations, which is mathematically quite involved. As a first step, this contribution therefore seeks to find solutions in terms of the system's mean field, which can be accurately described by the Gross-Pitaevskii equation (GPE) in three dimensions. However, finding optimal solutions of 3D problem as presented by Mennemann et al. (2015) is computationally very expensive.

The highly elongated setting exhibits a coupling of the transversal and longitudinal dynamics since atomic interactions lead to a transversal broadening of the gas. Nevertheless, one can effectively describe the resulting longitudinal mean-field dynamics of the Bose gas by a one-dimensional non-polynomial Schrödinger equation (NPSE), e.g., as derived in Salasnich et al. (2002). Since this nonlinearly affects the local propagation speed of excitations, it needs to be taken into account for optimal control solutions. While methods to create arbitrary (time-varying) optical 1D potentials have been presented recently by Deutschmann-Olek et al. (2022) with first experimental results by Calzavara et al. (2022), simple optical box potentials are feasible with state-of-the-art algorithms presented in Tajik et al. (2019).

This paper investigates optimal control solutions for the longitudinal dynamics of a quasi-1D Bose gas described by the non-polynomial Schrödinger equation, which is briefly

introduced in Section 2. After introducing the optimal control problem, Section 3 extends existing approaches for the 1D GPE given in Winkel and Borzi (2008) to the required npSE. Section 4 applies these solutions to optimally compress a Bose gas in a box potential and compares the resulting solution to simple basis-function approaches. Resulting conclusions and a short outlook are finally given in Section 5.

2. MEAN-FIELD DYNAMICS OF QUASI-1D BOSE GASES

We consider a cloud of N ultra-cold atoms trapped in a highly elongated trap with a tight transversal confinement due to the static parabolic potential $V_{\perp}(x, y) = \frac{\omega_{\perp}}{2}(x^2 + y^2)$, with the transversal angular frequency ω_{\perp} . Along the weakly confined longitudinal direction $z \in \mathcal{D} = [-L/2, L/2]$, a tunable potential $V(z, t)$ is created using spatially shaped light fields. We assume that the condensate remains in a Gaussian state close to the ground state in transversal direction, as illustrated in Fig. 1, which is the case for sufficiently low temperatures T , i.e., $k_{\text{B}}T < \hbar\omega_{\perp}$ with the Boltzmann constant k_{B} and the reduced Planck constant \hbar .

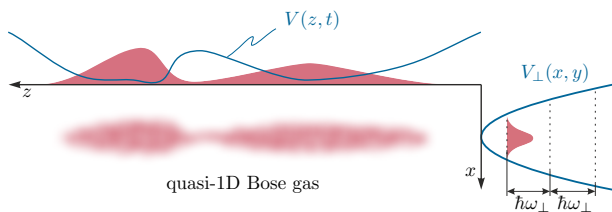


Fig. 1. Density ρ of an elongated atomic cloud with tight transversal confinement due to the static trapping potential $V_{\perp}(x, y)$ of the atom chip. Using spatially shaped attractive or repulsive light fields to create an additional optical dipole potential, one can generate complex time-varying longitudinal potentials $V(z, t)$.

The dynamics of the resulting cigar-shaped quasi-1D condensate of N particles can be effectively described by a non-polynomial Schrödinger equation (npSE) (see, e.g., Salasnich et al. (2002)) for its longitudinal wave function $\Psi(z, t)$ in normalized form

$$i\partial_t\Psi(z, t) = -\frac{1}{2m}\partial_{zz}\Psi(z, t) + V(z, t)\Psi(z, t) + \omega_{\perp}\left(\frac{1 + 3a_s N|\Psi(z, t)|^2}{\sqrt{1 + 2a_s N|\Psi(z, t)|^2}} - 1\right)\Psi(z, t), \quad (1)$$

with the (normalized) mass m , the transversal scattering length a_s and the transversal angular frequency ω_{\perp} given by the (normalized) transversal potential $V_{\perp}(x, y)$. The probability density $\rho(z, t)$ of finding a particle of the atomic cloud at position z and at time t can be obtained by $\rho(z, t) = |\Psi(z, t)|^2$ and thus

$$\int_{\mathcal{D}} |\Psi(z, t)|^2 dz = 1. \quad (2)$$

It is further assumed that $V(z, t)$ is sufficiently large at the domain boundaries such that $\Psi(\pm L/2, t)$ and $\partial_z\Psi(\pm L/2, t)$ vanishes.

3. OPTIMAL CONTROL OF THE NON-POLYNOMIAL SCHRÖDINGER EQUATION

We assume that the spatial shape of the longitudinal potential $V(z, t)$ can be parametrized by some control parameter $\lambda(t) \in \mathcal{V}$, which is element of a suitable function space \mathcal{V} . The longitudinal potential is thus given by $V(z, t) = V_{\lambda}(z, \lambda(t))$, where the subscript highlights the dependence on λ and thus implicitly on the time t .

The aim of this section is to find trajectories $\lambda(t)$ that transfer the npSE from an initial state $\Psi_0(z) = \Psi(z, 0)$, which is assumed to be the ground state of the initial potential $V(z, 0)$, to a desired state $\Psi_{\text{des}}(z)$ at time T . While this can be an arbitrary state in general, we restrict ourselves to ground states of the final potential $V(z, T)$. We thus seek for what is commonly referred to as a "shortcut to adiabaticity", e.g., Campo and Boshier (2012).

It is in general unclear if a trajectory for λ exists such that the final state reaches $\Psi(z, T) = \Psi_{\text{des}}(z)$ exactly or whether this control problem is solvable within a given time horizon T . Therefore, the existing literature (e.g., Winkel and Borzi (2008); Grond et al. (2009)) applies optimal control theory, where the optimality of such a transition is evaluated by a cost functional $J : \mathcal{V} \rightarrow \mathbb{R}$ in Bolza form

$$J(\lambda) = \phi(T, \Psi(z, T)) + \int_0^T l(t, \Psi(z, t), \lambda(t)) dt, \quad (3)$$

with the terminal costs $\phi(T, \Psi(z, T))$ and the integral costs $l(t, \Psi(z, t), \lambda(t))$ during the transition. An optimal trajectory¹ $\hat{\lambda}(t)$ is thus given by the constrained optimization problem

$$\min_{\lambda(\cdot)} J(\lambda) \quad (4a)$$

$$\text{s.t. } i\partial_t\Psi(z, t) = f(\Psi(z, t), \lambda(t)), \quad (4b)$$

$$\Psi(z, 0) = \Psi_0(z), \quad (4c)$$

$$\lambda(0) = \lambda_0, \lambda(T) = \lambda_T, \quad (4d)$$

where $f(\Psi(z, t), \lambda(t))$ is used as an abbreviation of the right-hand side of (1).

3.1 State and energy cost functionals

A typical choice of the cost functional $J(\lambda)$ evaluates the difference between the obtained final state $\Psi(z, T)$ and the desired state $\Psi_{\text{des}}(z)$, i.e.,

$$J_s = \frac{1}{2} \left(1 - \left| \int_{\mathcal{D}} \Psi_{\text{des}}^*(z) \Psi(z, T) dz \right|^2 \right) + \frac{\gamma_{\text{reg}}}{2} \int_0^T (\partial_t \lambda(t))^2 dt, \quad (5)$$

with $\gamma_{\text{reg}} > 0$ and the complex conjugate $(\cdot)^*$. The term $\frac{\gamma_{\text{reg}}}{2} \int_0^T (\partial_t \lambda(t))^2 dt$ penalizes strong variations of $\lambda(t)$ to regularize the optimization problem, improve the convergence (see Winkel and Borzi (2008)) and ensure smooth trajectories of λ which are favorable for experimental implementation.

¹ Variables at the optimum are marked with a hat, which is not to be confused with operators in quantum mechanics.

If the desired state $\Psi_{\text{des}}(z)$ is the ground state of the final potential $V(z, T)$, one can alternatively consider the energy-based cost functional of the form

$$J_e = \int_{\mathcal{D}} \mathcal{H}(\Psi(z, T)) dz - J_{e, \text{des}} + \frac{\gamma_{\text{reg}}}{2} \int_0^T (\partial_t \lambda(t))^2 dt, \quad (6)$$

with $\gamma_{\text{reg}} > 0$ and

$$J_{e, \text{des}} = \int_{\mathcal{D}} \mathcal{H}(\Psi_{\text{des}}(z, T)) dz \quad (7)$$

using the Hamiltonian density, see Erne (2018),

$$\mathcal{H}(\Psi(z, t)) = -\frac{1}{2m} \Psi^*(z, T) \partial_{zz} \Psi(z, t) + V_\lambda(z, \lambda_T) |\Psi(z, t)|^2 + \omega_\perp \sqrt{1 + 2a_s N |\Psi(z, t)|^2} |\Psi(z, t)|^2. \quad (8)$$

Since the ground state is by definition the state of lowest energy, both the state and the energy cost functionals have the same global minimum in this case. Note that both cost function have the same value at this global minimum by construction in the absence of degenerate states. The convergence behavior of the two cost functionals, however, can still differ substantially, as we will see in Section 4.

3.2 Optimality conditions

To find the optimal trajectory $\hat{\lambda}(t)$ without restricting the search space apriori, one can apply methods from the calculus of variations to obtain a set of equations that are necessary conditions for optimality (sometimes called optimality system). Using the Gâteaux derivative with respect to the control parameter

$$\delta J(\lambda; \xi_\lambda) = \frac{d}{d\nu} J(\lambda + \nu \xi_\lambda)|_{\nu=0} \quad (9)$$

where $\xi_\lambda \in \mathcal{V}$ is a variation of λ , a minimum of $J(\lambda)$ has to meet the first-order optimality condition

$$\delta J(\hat{\lambda}; \xi_\lambda) = 0 \quad (10)$$

for all admissible variations ξ_λ observing the boundary conditions (4d). Note that the cost functional J depends on the wave function $\Psi(z, t)$ and thereby on the control parameter through the system dynamics (1).

A commonly used approach is to follow the method of Lagrangian multipliers by introducing the Lagrange functional

$$L(\lambda, \Psi, p) = \phi(T, \Psi(z, T)) + \int_0^T l(t, \Psi(z, t), \lambda(t)) dt \quad (11)$$

$$+ \text{Re} \left\{ \int_0^T \int_{\mathcal{D}} p^*(z, t) (\partial_t \Psi(z, t) - f(\Psi(z, t), \lambda(t))) dz dt \right\},$$

which uses the system dynamics (4b) together with the adjoint variable $p(z, t)$. With this definition, the condition (10) is equivalent to vanishing (partial) Gâteaux derivatives of $L(\lambda, \Psi, p)$ with respect to λ , Ψ , and p (cp. Winckel and Borzì (2008)), i.e.,

$$\delta_p L(\lambda, \Psi, p; \xi_p) = 0 \quad (12a)$$

$$\delta_\Psi L(\lambda, \Psi, p; \xi_\Psi) = 0 \quad (12b)$$

$$\delta_\lambda L(\lambda, \Psi, p; \xi_\lambda) = 0 \quad (12c)$$

for all admissible variations ξ_λ , ξ_p , and ξ_Ψ .

Calculating (12) for all admissible variations regarding the boundary conditions (4c) and (4d), using the assumption

that $V(z, t)$ is sufficiently large such that $\Psi(\pm L/2, t) = \partial_z \Psi(\pm L/2, t) = 0$, and applying the fundamental lemma of the variational calculus, we obtain the optimality system for the optimization problem (4) as

$$i \partial_t \hat{\Psi}(z, t) = f(\hat{\Psi}(z, t), \hat{\lambda}(t)) \quad (13a)$$

$$i \partial_t \hat{p}(z, t) = \left(-\frac{1}{2m} \Delta + V_\lambda(z, \hat{\lambda}(t)) + A(\hat{\Psi}) \right) \hat{p}(z, t) + B(\hat{\Psi}) \hat{p}^*(z, t) \quad (13b)$$

$$\gamma_{\text{reg}} \partial_{tt} \hat{\lambda}(t) = -\text{Re} \left\{ \int \hat{\Psi}^*(z, t) \frac{\partial V_\lambda}{\partial \lambda} \right\} \Big|_{\lambda=\hat{\lambda}(t)} p(z, t) dz \quad (13c)$$

whereby

$$A(\Psi) = \omega_\perp \left(\frac{1 + 6a_s N |\Psi(z, t)|^2}{\sqrt{1 + 2a_s N |\Psi(z, t)|^2}} - 1 - \frac{(1 + 3a_s N |\Psi(z, t)|^2) a_s N |\Psi(z, t)|^2}{(1 + 2a_s N |\Psi(z, t)|^2)^{\frac{3}{2}}} \right)$$

$$B(\Psi) = \omega_\perp \left(\frac{3a_s N \Psi(z, t)^2}{\sqrt{1 + 2a_s N |\Psi(z, t)|^2}} - \frac{(1 + 3a_s N |\Psi(z, t)|^2) a_s N \Psi(z, t)^2}{(1 + 2a_s N |\Psi(z, t)|^2)^{\frac{3}{2}}} \right).$$

The boundary conditions for (13a) and (13c) are given by

$$\hat{\Psi}(z, 0) = \Psi_0(z), \quad (13d)$$

$$\hat{\lambda}(0) = \lambda_0, \quad \hat{\lambda}(T) = \lambda_T. \quad (13e)$$

The remaining terminal condition for the adjoint variable $p(z, t)$ at $t = T$ is given by either

$$\hat{p}(z, T) = i \Psi_{\text{des}}(z) \int_{\mathcal{D}} \Psi_{\text{des}}^*(z) \hat{\Psi}(z, T) dz \quad (13f)$$

when using the state cost functional J_s in (5) or by

$$\hat{p}(z, T) = -2i \left[-\frac{1}{2m} \Delta + V_\lambda(z, \lambda_T) + \omega_\perp \left(\frac{1 + 3a_s N |\hat{\Psi}(z, T)|^2}{\sqrt{1 + 2a_s N |\hat{\Psi}(z, T)|^2}} + 1 \right) \right] \hat{\Psi}(z, T) \quad (13g)$$

when using the energy cost functional J_e in (6), respectively. Note that solutions of (13) only guarantee local optimality and suitable globalization strategies can be applied if needed.

3.3 Solution of the optimality system

The respective optimality system can be solved using a gradient-based approach analogous to Winckel and Borzì (2008). Therefore, a gradient ∇J_λ is defined to meet

$$(\nabla J_\lambda, \xi_\lambda)_X = \delta J(\lambda; \xi_\lambda) \quad (14)$$

for all admissible directions $\xi_\lambda \in X$ and the inner product $(\cdot, \cdot)_X$ of the inner-product space X . Typical choices include the Sobolev H^1 or the Lebesgue L^2 space using $(a, b)_{L^2} = \int_0^T a(t) b(t) dt$ and $(a, b)_{H^1} = \int_0^T \partial_t a(t) \partial_t b(t) dt$. Following Winckel and Borzì (2008), using H^1 yields less oscillating and more robust solutions with respect to the choice of γ_{reg} while also attaining better cost-value results

in less computation time. For this reason, $X = H^1$ chosen as inner product space in this work.

Since $\delta J(\lambda; \xi_\lambda) = \delta_\lambda L(\lambda, \Psi, p; \xi_\lambda)$ if (12a) and (12b) vanish, (14) results in a Poisson equation for $\nabla J_\lambda(t)$, i.e.

$$\frac{d^2}{dt^2} \nabla J_\lambda(t) = \gamma_{\text{reg}} \ddot{\lambda}(t) + \text{Re} \left\{ \int_{\mathcal{D}} \Psi^*(z, t) \frac{\partial V_\lambda}{\partial \lambda} p(z, t) dz \right\}, \quad (15a)$$

with the boundary conditions

$$\nabla J_\lambda(0) = 0, \quad \nabla J_\lambda(T) = 0. \quad (15b)$$

To obtain numerical solutions, the system dynamics (13a) and the adjoint dynamics (13b) together with the terminal condition (13f) or (13g), respectively, are solved by forward and backward integration starting from an initial guess of the control parameter $\lambda(t)$. This is done by employing a Crank-Nicolson scheme. Note that the implicit nature of the Crank-Nicolson scheme requires that a nonlinear system of equations is solved in each time step for the nonlinear state dynamics (13a) unlike for the linear adjoint dynamics (13b). With the values of Ψ and p from the forward and backward integration, the two-point boundary value problem (15) can be solved directly by spatial discretization. Note that ∇J_λ vanishes at time $t = 0$ and $t = T$ and thus is an admissible variation of the boundary conditions (4d). This is a feature of the H^1 space and would not be the case in the L^2 space setting, see Winkel and Borzi (2008). With the obtained gradient $\nabla J_\lambda(t)$, Quasi-Newton (BFGS) iterations are performed until $\|\nabla J_\lambda\|_X$ is below a certain tolerance or a maximum number of iterations is reached.

4. MEAN-FIELD OPTIMAL COMPRESSION IN OPTICAL BOX POTENTIALS

While optical potentials can be arbitrarily shaped in principle, the large number of experimental iterations required by existing heuristic approaches, see, e.g., Tajik et al. (2019), limits their usability for dynamic (i.e., time-varying) applications. However, these methods can be utilized to create optical box potentials by statically compensating for potential roughnesses of the bottom of the box while only dynamically moving the walls, which is easily possible. In the following, we want to illustrate the presented results for the compression of a quasi-1D Bose gas, which is a fundamental operation of a quantum field thermal machine.

Since the steepness of optical box potentials is limited by the finite optical aperture, we assume that a box potential of initial length $w_0 < L$ is given by

$$V_\lambda(z, \lambda(t)) = V_{\text{max}} - \frac{V_{\text{max}}}{2} \text{erf} \left(\frac{z + (w_0/2 - \lambda(t))}{\sigma} \right) + \frac{V_{\text{max}}}{2} \text{erf} \left(\frac{z - (w_0/2 - \lambda(t))}{\sigma} \right) \quad (16)$$

using the Gaussian error function $\text{erf}(z)$ with $\sigma = 3 \mu\text{m}$, which is consistent with current experimental setups. Here, $\lambda(t)$ represents the displacement of the wall acting symmetrically on both sides as illustrated in Fig. 2. For a final displacement λ_T , the resulting compression ratio is given by $r_{\text{comp}} = \frac{w_0 - 2\lambda_T}{w_0}$.

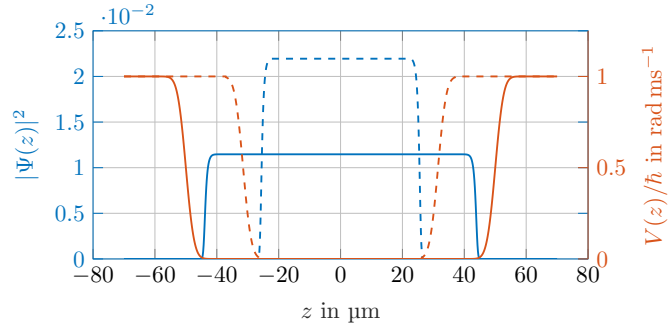


Fig. 2. Initial and final potential and the density profiles of the corresponding ground states for the compression of a condensate from $100 \mu\text{m}$ to $50 \mu\text{m}$, i.e., $r_{\text{comp}} = 0.5$.

In the absence of an elaborate optimal control solution, experiments are typically performed using simple linear ramps for the control parameter, i.e.,

$$\lambda_{\text{lin}}(t) = \begin{cases} \lambda_0 + \frac{t}{T}(\lambda_T - \lambda_0) & t \in [0, T] \\ \lambda_T & t \geq T, \end{cases} \quad (17)$$

to achieve a dynamic transition of the applied potential.

Dynamic changes of the control parameter λ create excitations of the density that propagate with finite velocity c_s usually called speed of sound. For the npSE, it is given by (see Erne (2018))

$$c_s^2 = \omega_\perp a_s N \rho \frac{2 + 3a_s N \rho}{m(1 + 2a_s N \rho)^{3/2}} \quad (18)$$

and assumes different values at each location z in general due to its dependence on the local atomic density ρ . Contrary to scenarios where the entire potential landscape is actuated, a moving potential walls approach solely relies on the condensate's dynamics to act on neighboring particles and adjust a desired state. As a result, the time horizon T for an optimal transition of the Bose gas cannot be shorter than the time it takes for excitations to reach the opposite wall of the box potential. The given scenario thus exhibits a minimum control time T_{min} similar to boundary control problems, see, e.g., Meurer (2013). To obtain a choice for T without exact results for the minimum control time, one can use the simple geometric estimate that

$$T_{\text{min}} \approx \frac{w_0}{c_{s,0}} \frac{1 + r_{\text{comp}}}{2}, \quad (19)$$

with the speed of sound $c_{s,0}$ corresponding to the initial flat density $\rho_0 = |\Psi_0|^2$ of the box potential. Note that this estimate ignores the fact that c_s increases with density and thus typically overestimates the true minimum control time in a compression scenario.

Using the parameter values from Tab. 2 and a compression ratio of $r_{\text{comp}} = 0.5$ yields $T_{\text{min}} \approx 45.96$ ms. Solving the optimality system (13) for the energy-based cost function (6) with $\gamma_{\text{reg}} = 1 \times 10^{-5}$ over a time horizon $T = 45$ ms yields the results shown in Fig. 3. For the initial trajectory $\lambda(t)$ in the optimization scheme a linear ramp (17) was chosen. After $t = T$, the control parameter λ is held constant to observe the evolution of the system state after the transition. The optimal transition is able to eliminate excitations when approaching T and ultimately ends up in the desired ground state of the compressed potential. From visual inspection alone one clearly sees that a shorter

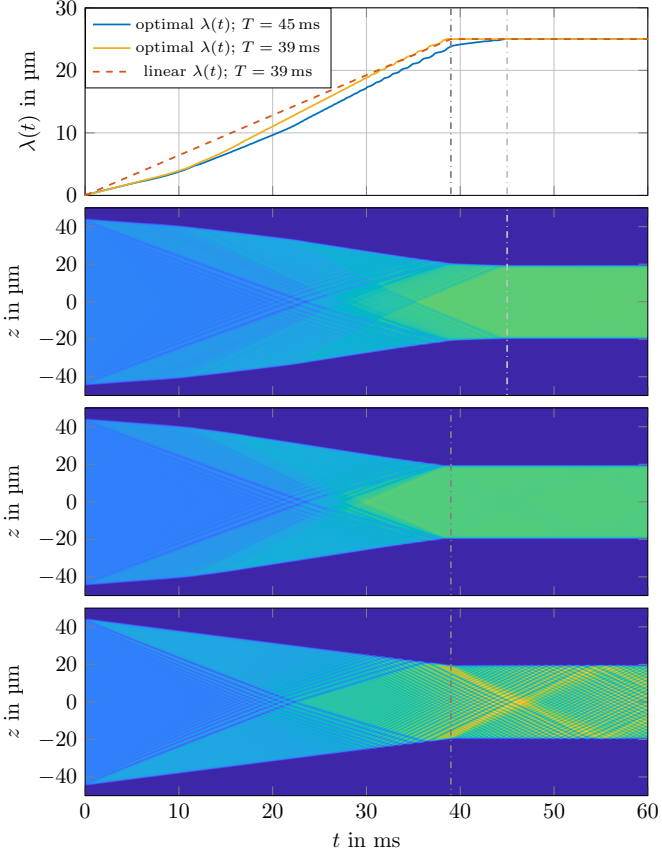


Fig. 3. Comparison of a compression with $r_{\text{comp}} = 0.5$ using a linear ramp (17) and optimal trajectories using the energy cost functional J_e for $T = 45$ ms and $T = 39$ ms. The top plot illustrates the evolution of the control parameter $\lambda(t)$. The corresponding evolution of the density $\rho(z, t)$ for the linear (optimal) trajectory of $\lambda(t)$ is shown in the plots below, whereby the optimal trajectories of $\hat{\lambda}(t)$ was determined by solving the optimality conditions (13) as described in Section 3.3.

time horizon is possible, which is verified by the optimal trajectory for $T = 39$ ms shown in Fig. 3. The evolution of the density for a linear transition using (17) is finally given for comparison. It is interesting to note that optimal solutions close to the true T_{min} yield particularly simple and smooth trajectories for $\hat{\lambda}(t)$.

A popular alternative in quantum control applications to the indirect optimization approach (IOA) of using the optimality conditions (13) is to directly restrict the function space of the control parameter \mathcal{V} using a finite number of basis functions. The optimal solution in this restricted space is then given by a simpler static optimization problem that does not use further information on the system (black-box optimization). Such a basis-function approach (BFA) can be quite powerful, e.g., by combining it with a randomisation of the basis functions, see Doria et al. (2011). For the desired transition between two steady states of the system, a particularly simple finite-dimensional parametrization of the control parameter is given by

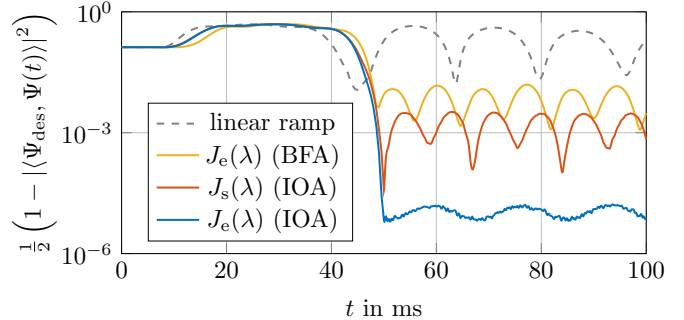


Fig. 4. Evolution of the L^2 -error $\frac{1}{2} (1 - |\langle \Psi_{\text{des}}, \Psi(t) \rangle|^2)$ of the system state $\Psi(t)$ of the resulting optimal $\hat{\lambda}(t)$ for different cost functionals $J_e(\lambda)$ and $J_s(\lambda)$ using the indirect optimization approach (IOA). The corresponding evolution when using a basis function approach (BFA) with $M = 4$ and a simple linear ramp $\lambda_{\text{lin}}(t)$ is given for comparison.

$$\lambda(t) = \begin{cases} \lambda_{\text{lin}}(t) + \sum_{k=1}^M a_k \sin\left(k\pi \frac{t}{T}\right) & t \in [0, T] \\ \lambda_{\text{lin}}(t) & \text{else.} \end{cases} \quad (20)$$

Due to the choice of harmonic basis functions on top of the linear ramp, the resulting static optimization problem is unconstrained apart from the system equation, i.e., the resulting $\lambda(t)$ is a feasible (smooth) trajectory for all possible coefficients a_k , $k = 1 \dots M$. To find the optimal coefficients a_k , one can use optimization algorithms that do not require (explicit) gradient information, which is essential for more involved quantum systems that are either impossible or difficult and time consuming to simulate. Together with the typically highly non-convex nature of the resulting static optimization problem, global optimization tools such as Bayesian or surrogate optimization methods are beneficial, see, e.g., Jones et al. (1998); Frazier (2018). Due to the comparatively fast simulation time of the npSE, a Quasi-Newton algorithm without gradient information is used.

To assess the resulting optimal control solutions for both cost functionals, i.e., state and energy costs, and indirect and basis function approaches, the evolution of the state error $\frac{1}{2} \left(1 - \left| \int_{\mathcal{D}} \Psi_{\text{des}}^*(z) \Psi(z, T) dz \right|^2\right)$ is illustrated in Fig. 4 for $r_{\text{comp}} = 0.25$ and $T = 45$ ms. As one can see, the optimal solution using the energy cost function J_e yields much better results. The reason for this is the significantly improved convergence behavior of J_e compared to using J_s , which holds true for the IOA as well as the BFA. A comparison of the obtained cost function values is given in Tab. 1. Not only are the required number of iterations N_{iter} until the algorithms converges significantly lower, but also the state costs J_s of solutions obtained using J_e are comparable or even lower than when using J_s itself during the optimization. The reduced search space somewhat limits the optimality of the resulting solutions and the achievable values of the cost function stagnate with an increasing number of basis functions, see Fig. 5, while the required number of iterations rises quickly.

5. CONCLUSIONS AND OUTLOOK

In this work, we presented an optimal control solution for the mean-field of a quasi-1D Bose gas that is described by a

	$J_e(\hat{\lambda})$	$J_s(\hat{\lambda})$	N_{iter}
linear ramp	2.9441×10^{-2}	1.9162×10^{-1}	1
BFA using J_e	6.2236×10^{-4}	8.9778×10^{-3}	65
BFA using J_s	2.7207×10^{-2}	2.4546×10^{-3}	155
IOA using J_e	1.5338×10^{-5}	6.7511×10^{-6}	277
IOA using J_s	5.3696×10^{-4}	3.7510×10^{-5}	535

Table 1. Comparison of optimal trajectories $\hat{\lambda}$ found using either the IOA or BFA approach evaluated at both cost functionals J_e and J_s . For the BFA, $M = 4$ was chosen.

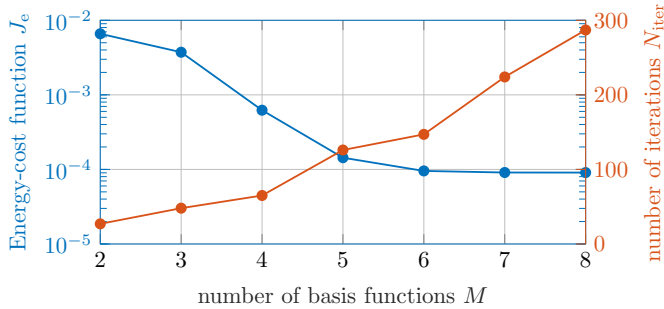


Fig. 5. Resulting optimal values of the energy cost function $J_e(\hat{\lambda})$ for different number of basis functions M and the required number of iterations N_{iter} of the numerical optimization algorithm.

Parameter	Value
normalized mass m	1.368
transversal frequency ω_{\perp}	1×10^1
scattering length a_s	4.2×10^{-3}
particle number N	5.0×10^3

Table 2. Typical experimental parameters normalized to time in ms and space in μm .

non-polynomial Schrödinger equation. Necessary optimality conditions for energy and state cost functionals were derived using a variational formulation and solutions of the resulting optimal system were used to optimally compress a quasi-condensate in an (optical) box potential. Energy cost functionals show superior convergence properties for the derived indirect optimization approach as well as for simple basis function approaches. The latter might be particularly useful beyond mean-field scenarios where accurate closed-form descriptions of the (stochastic) system dynamics are hardly available. Due to the particularly simple and smooth solutions for optimal choices of the time horizon, one could further include T in the optimization for a tailored set of basis functions.

ACKNOWLEDGEMENTS

This research was funded in part by the Austrian Science Fund (FWF) [P36236] and the DFG Research Unit FOR 2724 on “Thermal machines in the quantum world” (FWF I-6047). Financed by the European Union - NextGenerationEU. S.E. acknowledges an ESQ (Erwin Schrödinger Center for Quantum Science and Technology) fellowship funded through the European Union’s Horizon 2020 research and innovation programme under the Marie Skłodowska-Curie grant agreement No 801110.

REFERENCES

- Calzavara, M., Kuriatnikov, Y., Deutschmann-Olek, A., Motzoi, F., Erne, S., Kugi, A., Calarco, T., Schmiedmayer, J., Prüfer, M., 2022. Optimizing optical potentials with physics-inspired learning algorithms. arXiv:2210.07776 [cond-mat].
- Campo, A. d., Boshier, M. G., 2012. Shortcuts to adiabaticity in a time-dependent box. *Scientific Reports* 2 (1), 648.
- Deutschmann-Olek, A., Calzavara, M., Schmiedmayer, J., Calarco, T., Kugi, A., 2022. Iterative shaping of optical potentials for one-dimensional bose-einstein condensates. In: 61st IEEE CDC. Cancun, pp. 5801–5806.
- Doria, P., Calarco, T., Montangero, S., 2011. Optimal Control Technique for Many-Body Quantum Dynamics. *Physical Review Letters* 106 (19), 190501.
- Dotsenko, I., Mirrahimi, M., Brune, M., Haroche, S., Raymond, J.-M., Rouchon, P., 2009. Quantum feedback by discrete quantum nondemolition measurements: Towards on-demand generation of photon-number states. *Physical Review A* 80 (1).
- Erne, S., 2018. Far-from-equilibrium quantum many-body systems: From universal dynamics to statistical mechanics. Ph.D. thesis, University of Heidelberg.
- Frazier, P. I., 2018. A Tutorial on Bayesian Optimization. arXiv:1807.02811 [cs].
- Grond, J., von Winckel, G., Schmiedmayer, J., Hohenester, U., 2009. Optimal control of number squeezing in trapped Bose-Einstein condensates. *Physical Review A* 80 (5), 053625.
- Jones, D. R., Schonlau, M., Welch, W. J., 1998. Efficient Global Optimization of Expensive Black-Box Functions. *Journal of Global Optimization* 13 (4), 455–492.
- Magrini, L., Rosenzweig, P., Bach, C., Deutschmann-Olek, A., Hofer, S. G., Hong, S., Kiesel, N., Kugi, A., Aspelmeyer, M., 2021. Real-time optimal quantum control of mechanical motion at room temperature. *Nature* 595 (7867), 373–377.
- Mennemann, J.-F., Matthes, D., Weishäupl, R.-M., Langen, T., 2015. Optimal control of Bose-Einstein condensates in three dimensions. *New Journal of Physics* 17 (11), 113027.
- Meurer, T., 2013. Control of Higher-Dimensional PDEs: Flatness and Backstepping Designs. Springer, Berlin.
- Oman, A., Levine, H., Keesling, A., Semeghini, G., Wang, T. T., Ebadi, S., Bernien, H., Zibrov, A. S., Pichler, H., Choi, S., Cui, J., Rossignolo, M., Rembold, P., Montangero, S., Calarco, T., Endres, M., Greiner, M., Vuletić, V., Lukin, M. D., 2019. Generation and manipulation of Schrödinger cat states in Rydberg atom arrays. *Science* 365 (6453), 570–574.
- Salasnich, L., Parola, A., Reatto, L., 2002. Effective wave equations for the dynamics of cigar-shaped and disk-shaped Bose condensates. *Physical Review A* 65 (4), 043614.
- Tajik, M., Rauer, B., Rauer, B., Schweigler, T., Cataldini, F., Sabino, J., Møller, F. S., Ji, S.-C., Mazets, I. E., Schmiedmayer, J., 2019. Designing arbitrary one-dimensional potentials on an atom chip. *Optics Express* 27 (23), 33474–33487.
- Winckel, G. v., Borzi, A., 2008. Computational techniques for a quantum control problem with H^{-1} -cost. *Inverse Problems* 24 (3), 034007.